Third International Conference on CFD in the Minerals and Process Industries
CSIRO, Melbourne, Australia
10-12 December 2003

CFD SIMULATION AND EXPERIMENTAL VALIDATION OF DILUTE PARTICULATE TURBULENT FLOWS IN A 90° DUCT BEND

Benny KUAN[1], William YANG[1,2] and Chris SOLNORDAL[1,2]

[1]CRC – Clean Power from Lignite, Mulgrave, Victoria 3170, AUSTRALIA
[2]CSIRO Minerals, Clayton, Victoria 3168, AUSTRALIA

ABSTRACT

Numerical simulations are performed for dilute gas-solid flows in a rectangular duct consisting of a horizontal-to-vertical bend. A very low solid mass loading is considered and the bend has a turning radius of 1.5 duct diameters. The flow scenario investigated corresponds to flow conditions downstream of the mill in the burner duct of a pulverized fuel (pf) fired lignite power plant. On the grounds of dynamic similarity, flow parameters in the calculation are selected to match the three dimensionless quantities, namely, particle Reynolds number, Stokes number and Froude number that characterise the industrial flow. Assuming all pf particles are spherical in shape, solution of the dispersed gas-solid flow is carried out using a commercial Computational Fluid Dynamics (CFD) package CFX-4.4. An Eulerian /Lagrangian approach that takes into account the effects of turbulent dispersion and pressure gradients is utilised for solving gaseous and particulate flow properties. Numerical predictions for the mean and turbulent gas flow properties, and particle velocities are validated against Laser Doppler Anemometry (LDA) measurements.

NOMENCLATURE

d	particle diameter
D	duct hydraulic diameter
F	force vectors acting on particle surface
k	turbulence kinetic energy
m	particle mass
R	elbow turning radius
r*	distance from duct outer wall normalised by D
s	streamwise distance
T	time scale
u	velocity vector
U	mean axial velocity
u’	fluctuating velocity
V	mean transverse velocity
W	channel width
ε	turbulence dissipation rate
θ	turning angle

INTRODUCTION

Elbows and bends are commonly used in pneumatic conveying systems to change flow direction so as to transport the suspended material to the desired delivery point within a limited space. In the case of coal-fired power plants that operate on a continuous supply of pulverised coal to furnaces, mal-distribution of pulverised fuel often occurs as coal particles are pneumatically transported from the mill through ducts consisting of numerous bends and straight sections.

Incorporation of 90° bends in a pneumatic conveying system also results in system pressure drop, duct erosion, and solids attrition. Motion of the suspended particles and their interactions with the carrier fluid and the confining surfaces in a bend are therefore very complex.

In a coal-fired power plant utilising lignite, the mill-duct system is typically constructed from ducting components of large diameter-to-length ratio. Particle ropes formed within the ductwork usually do not have sufficient straight duct length downstream to fully disperse and form a homogeneous fuel-air mixture prior to the bifurcation that is designed to split the fuel flow. This invariably makes it difficult for the plant operators to accurately control the amount of pf supply to individual burners and hence maintain an optimal combustion condition inside the furnace.

Furthermore the non-uniform distribution of fuel across ducts severely complicates the measurement of fuel flow rate. Various sensing techniques have been developed by researchers (Yan *et al*., 1995; Millen *et al*., 2000; Ma and Yan, 2000; Barratt *et al*., 2000) to facilitate on-line measurement of solids mass flow rate in mill-ducts, however, none of them have so far been proven to work adequately for mill-duct flows subject to substantial particle roping.

In an effort to gain a better understanding of solid mal-distribution inside mill-duct systems, the CRC-Clean Power from Lignite has funded a project to develop a generic mill-duct flow model based on CFD simulation as well as direct flow measurement performed in the Advanced Laser Diagnostic Laboratory at CSIRO-Minerals. The model, after it has been validated against laboratory measurements, is intended to serve as a tool for optimising mill-duct design and operation.

The current study forms part of this CRC-funded project and it is an extension to an earlier numerical study, which simulates some of the published single- and two-phase flow experiments involving a 90° duct bend (Kliafas and Holt, 1985; Yilmaz and Levy, 1998; Sudo *et al*., 2001). At the present stage, the primary objective is to validate a CFD model in its capability for predicting single and two-phase mill-duct flows in a 90° bend. In all two-phase flow calculations, gas turbulence is solved with either a Differential Reynolds Stress Model (DRSM) or the standard k-ε turbulence model. For the solid phase, particle tracks are predicted through a Lagrangian

approach taking into consideration of one-way coupling, turbulence dispersion, and pressure gradient effects.

Model validation makes use of experimental data that are directly obtained from laboratory tests utilising a 3D laser diagnostic technique, namely, Laser Doppler Anemometry (LDA). Flow measurements, including mean and instantaneous gas and solid velocities, turbulence intensities, and particle size distributions, are performed. The measurements form a comprehensive database from which a direct comparison with numerical results can be made.

TEST FACILITY

A schematic sketch of the entire test facility is shown in Fig. 1. It features an open-circuit suction wind tunnel where the airflow is drawn into the system by means of a centrifugal fan through an entry piece that consists of an elliptical bell-mouth inlet and a honeycomb flow straightening section. The air then passes through a converging nozzle to attain a higher velocity before entering into the test section. Design of the converging nozzle follows Borger's contractor profile (Borger, 1973) to ensure flow uniformity within ±0.5%.

The square-sectioned (150 mm × 150 mm) test section is constructed using 10 mm thick Perspex sheets, and the main components of the test facility include a 3.5 m horizontal straight duct, a 90° bend with a turning radius of 225 mm and a 1.8 m vertical straight duct.

Glass spheres with an average diameter of 66μm are released into the gas flow field from a fluidised-bed feeder. Solid/gas mass loading ratio reached is well below 1% so as to set up a dilute gas-solid flow regime inside the test section.

All measurements are performed at the test section centre plane at various streamwise stations. At each station, flow measurements are carried out as close as 1 mm from the duct walls.

A baghouse dust collector is connected upstream to the centrifugal fan to remove dispersed particles in the outgoing gas-solid flow before it is discharged into the atmosphere.

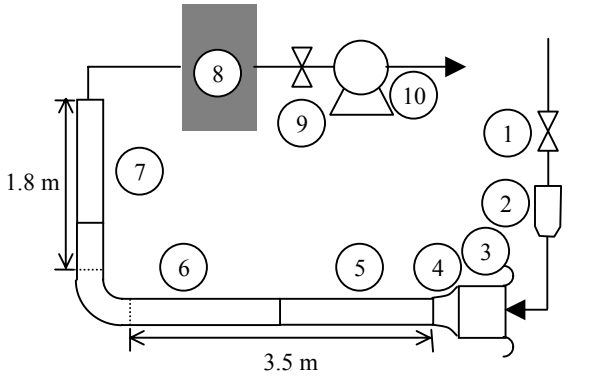

1	Feeder valve	6	90° duct bend
2	Fluidised bed feeder	7	Vertical straight duct
3	Bell mouth entry	8	Baghouse dust collector
4	Converging duct	9	Fan controller
5	Horizontal straight duct	10	Centrifugal fan

Figure 1: Experimental flow system

FLOW CONDITIONS MODELLED

Compared to the experimental geometry outlined above, the elbow duct considered in the numerical calculations only extends 10D upstream and 12.75D downstream. Measured upstream flow properties, including mean axial gas velocity, turbulence intensities, and particle velocities have been used as inlet conditions. The underlying bulk gas velocity U_b is set to 10 m/s and corresponding values for the dynamic similarity parameters are provided in Table 1. Also presented in the table are some important flow statistics and dynamic similarity parameters specific to mill-duct flows upstream of an industrial bifurcation. Fig. 2 depicts one such industrial flow and a simplified flow scenario that is currently being studied in the laboratory. In Table 1, parameters in each column are further categorised into those pertaining to flows in the curved as well as straight ducts. Definitions of these parameters are given below:

$$\mathrm{Re} = \frac{\rho_f U_b D}{\mu} \tag{1}$$

$$\mathrm{Re}_p = \frac{\rho_f V_T d_p}{\mu} \tag{2}$$

$$\mathrm{St} = \frac{\rho_p d_p^2 \mathrm{Re}}{\rho_f (R_o) D} \tag{3}$$

$$\mathrm{Fr} = \frac{\rho_f U_b^2}{\rho_p d_p g} \tag{4}$$

Re_p denotes particle Reynolds number; St is a modified version of Fan and Zhu (1998)'s particle Stokes number; Fr is Froude number for gas-solid flows; V_T denotes particle terminal velocity; U_b is fluid's bulk velocity based on fluid mass flow rate and duct cross-section area. The presently adopted Stokes number (3) is defined as a ratio

Table 1: Summary of essential flow parameters

Flow	90° bend		Upstream bifurcation	
	Curved section	Straight section	Curved section	Straight section
Geometry				
R_o [m]	0.3	-	3.0	-
l [m]	-	1.8	-	3.68
D [m]	0.15	0.15	1.27	1.76
Gas phase				
U_b [m/s]	10.0	10.0	28.6	28.6
ρ_f [kg/m^3]	1.2	1.2	0.78	0.78
μ [kg/ms]	1.8E-5	1.8E-5	1.95E-5	1.95E-5
Solid phase				
L_p			0.1	0.1
ρ_p [kg/m^3]	2500	2500	1400	1400
d_p [μm]	66	66	80	80
V_T [m/s]	0.28	0.28	0.22	0.22
Dynamic similarity				
Re	1.0E5	1.0E5	1.45E6	2.01E6
Re_p	1.26	1.26	0.704	0.704
St	19.8	3.29	4.22	3.55
Fr	75.7	75.7	581	581

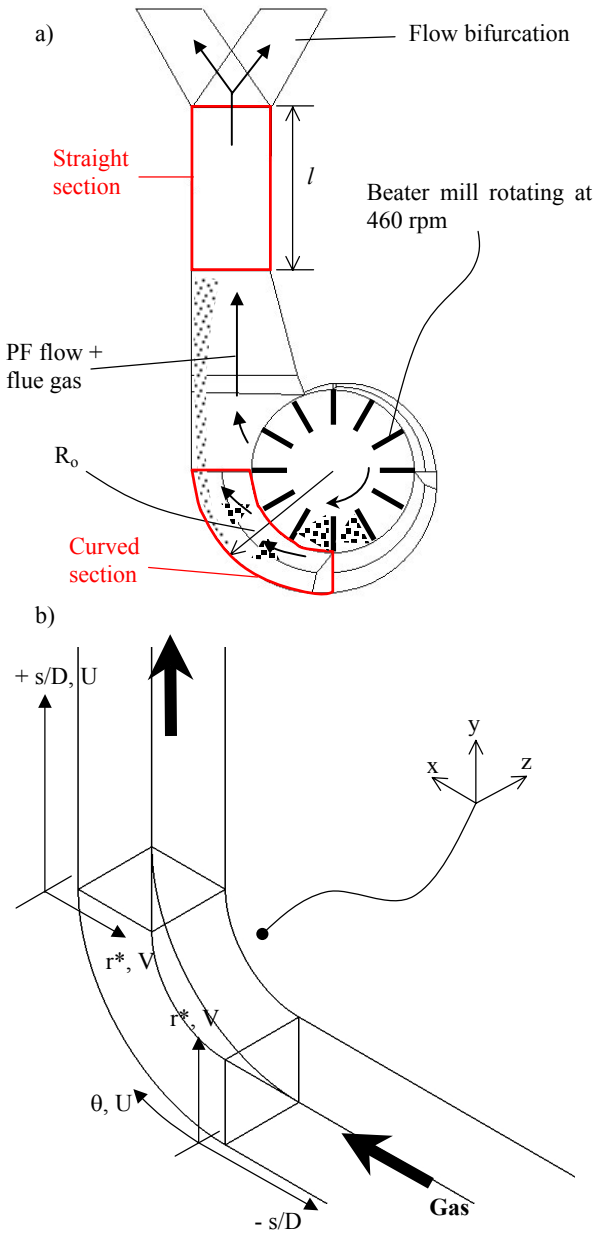

Figure 2: a) Schematic representation of an industrial flow regime; b) Flow configuration tested in the laboratory

between particle relaxation time and fluid's response to a change in bulk flow direction. For straight flows, outer-wall turning radius R_o in (3) should thus be replaced by duct length l.

Of the four dynamic similarity parameters listed in Table 1, St is one of the most critical factors for characterising particle motion in a curved flow field; a higher St indicates a collision-oriented particulate flow motion. Good agreement in St is observed for straight flows downstream from the elbow and upstream of the mill bifurcation. Particle behaviours in these regions are thus expected to display similar trends.

In contrast, the Froude number evaluated for the two cases differ drastically. This simply implies a predominance of inertial effects over gravity on particle motion as all calculated Froude numbers Fr are substantially greater than unity.

NUMERICAL METHODS

Gas-phase

Local mean gas flow properties, such as velocity and turbulence kinetic energy, are calculated numerically for the considered turbulent flow field by solving a set of Reynolds-averaged Navier-Stokes partial differential equations using CFX4.4. Reynolds stresses are either directly modelled from their own transport equations (Differential Reynolds Stress Modelling or DRSM) or through the well-known Boussinesq relation for isotropic turbulence. The later methodology is applied in conjunction with the standard k-ε turbulence model (Launder and Spalding, 1974).

Solid-phase

Instantaneous positions and velocities of the dispersed phase are solved from a set of ordinary differential equations with the local frame of reference fixed to the centre of individual particles. This approach is known as the Lagrangian particle tracking method. Motion of particles suspended in a continuous fluid is determined by numerically integrating the equations of motion for the dispersed phase in a fluid flow. The equation of particle motion may be expressed as

$$m_p \frac{d\mathbf{u}_p}{dt} = \mathbf{F}_D + \mathbf{F}_g + \mathbf{F}_{pg} + \mathbf{F}_A \qquad (5)$$

where subscript p represents particle properties and subscripts D, g, pg, and A respectively denote force components arising from drag, gravity, flow pressure gradient, and added mass effect. A detailed description of mathematical models for the force components considered in (5) is available from Fan and Zhu (1998), and Huber and Sommerfeld (1998).

In order to solve the equation of motion (5) for every particle track in the flow domain, instantaneous fluid velocity components at all particle locations need to be determined in advance. It is through the inclusion of these instantaneous fluid velocity components that the effects of turbulence are manifest in the calculation of particle motions. The present work adopts a classical stochastic approach by Gosman and Ioannides (1981) for the estimation of fluid fluctuating velocities. Subsequent particle track integration is carried out over an interaction time that is the minimum of two time scales, namely, eddy lifetime and particle transit time.

All calculations are carried out on a 80×80×135 (Y×Z×s) grid which consists of only hexahedral cells.

RESULTS

Gas-phase

Three separate gas flow calculations were performed either on the basis of a fully-developed turbulent upstream condition or flow data measured at 7D prior to the elbow inlet. Compared to the simulation result, laboratory measurements clearly indicate the gas flow has not yet reached a fully-developed state in the upstream horizontal duct. As is shown in Table 2, both boundary layer

thickness ($\delta_{99\%}$) and mean centreline flow velocity raise gradually towards the elbow inlet. The boundary layer growth seems to stabilise at s/D = -1.0 while at the same time the mean velocity profile becomes slightly skewed towards the inner wall. This may point to a possible upstream influence by the 90° bend that is located at s/D = 0.0.

Table 2: Boundary-layer properties upstream of the bend

S/D	$\delta_{99\%}$ [mm]	U_c/U_b
-11.0	49	1.18
-7.0	55	1.22
-3.0	64	1.23
-1.0	64	1.25

Mean flow properties at selective stations are presented in Fig. 3 and 4 on the basis of local coordinate systems already defined in Fig. 2.

As can be observed from the mean velocity profiles at the duct centre plane, effects of inlet conditions and turbulence models on the numerical predictions are not as extensive as one would expect. However, use of the DRSM does result in a more realistic representation of the flow recovery process at the inner wall downstream from the bend, particularly at θ = 90° and s/D = 1.0. Further away from the bend exit, the gas flow gradually evolves towards a fully-developed turbulent structure. However, neither of the turbulence models is able to capture this phenomenon accurately.

Interestingly, the predicted downstream flow pattern is also sensitive to changes in the prescribed inlet conditions, even though both sets of numerical data display similar characteristics in their upstream velocity profiles.

In addition to the mean gas flow field at the centre plane, LDA measurement of the fluctuating gas velocity components is also available for model validation and the results are presented in Fig. 4. In view of the fact that the gas flow entering into the testing facility is still under-developed, profiles in Fig. 4 indicate a less turbulent core that gradually diminishes towards the first half of the bend. The present DRSM prediction is unable to reflect this because it is based on fully-developed inlet conditions.

A short distance downstream from the bend, a sharp peak in the u' profile (s/D = 1.0) suggests a rising dominance of turbulent mixing in the flow field. This is a result of flow entrainment between the fast-moving gas stream originated from the outer wall and the slow gas close to the inner wall. Unlike the level of agreement that could be achieved for the mean gas flow, application of DRSM only leads to a good qualitative prediction of the underlying turbulence structure. Quantitatively, the predicted turbulent fluctuation could be as low as 60% of the measured value. This contributes to a major source of error for subsequent particle tracking calculations, which require the knowledge of the local turbulence time scale T (=k/ε).

Solid-phase

Assuming solid motion has negligible influence on the

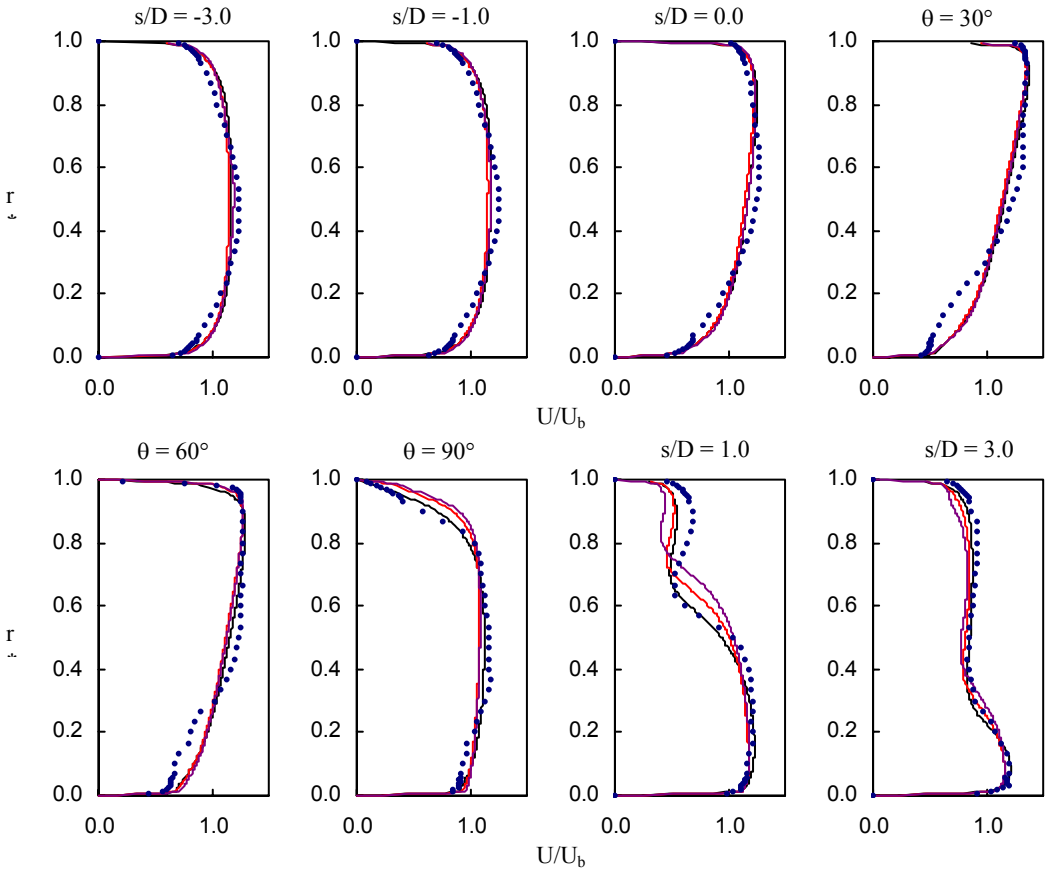

Figure 3: Normalised mean axial gas velocity profiles at duct centre plane (• experiment; — DRSM + fully-developed inlet; — standard k-ε model + fully-developed inlet; — standard k-ε model + measured inlet)

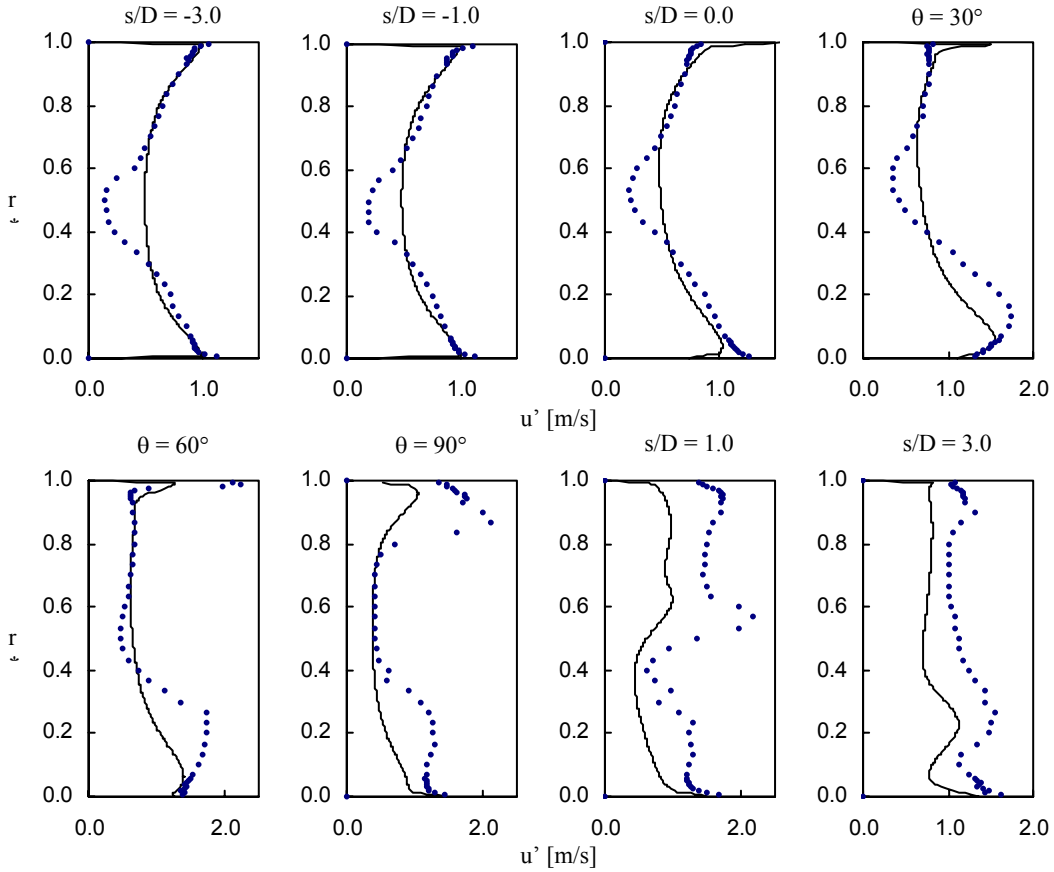

Figure 4: Fluctuating axial velocity profiles at duct centre plane (• experiment; — DRSM + fully-developed inlet)

background gas turbulence structure, Lagrangian particle tracking with one-way coupling is applied to solve particle dynamics within the elbow duct. A total of 10,000 particle tracks are considered in the calculations and two separate runs are carried out: one based on a uniform particle inlet velocity; the other assuming particles follow a fully-developed velocity profile at the duct inlet. In each case, the prescribed particle inlet velocity is offset by a small increment u'_p to account for any possible perturbations in particle motion. At present, u'_p is chosen to vary randomly between –0.5 and 0.5 m/s, which roughly corresponds to u' at the duct core at s/D = 10.0.

Measured and calculated mean particle velocities are presented in Fig. 5. In general, numerical results compare favourably with the data, except in regions close to the outer wall upstream and 30° into the bend. At these locations, the calculated particle velocity tends to exceed the measured values by as much as 70%. One possible explanation to this disparity would be that the particles are much better suspended in the experiment than they are in the calculation. Chances of particles impacting onto the outer wall are thus greatly reduced. Near-wall particles in the experiment are then able to closely follow the gas flow pattern. This may be related to a deficiency in the turbulent dispersion model used. Over-prediction of near-wall mean gas velocity (see Fig. 3) is also another major contributor to this disparity.

Within the second half of the bend, particle tracks become extinct in the vicinity of the inner wall as the particles, under the influence of their own inertia, separate from the turning fluid flow. In contrast, LDA is still able to pick up particles passing through this region though at a lower data rate. Further downstream, more particles are being thrown towards the confining walls by a pair of counter-rotating vortices inside the duct. However, a more uniform distribution of particle tracks is restored at s/D = 3.0. At this location, the calculated particle velocities exhibit good agreement with the measured data.

CONCLUSION

Two-phase LDA measurements as well as numerical simulations are performed for a 90° duct bend. The experimental data has been applied to validate the result of a CFD simulation in an effort to identify areas where further work is necessary to improve the accuracy of numerical prediction for flows with dilute solid suspension. The present study has found:

1. Gas-phase flow prediction downstream from the elbow is sensitive to variations in the prescribed inlet condition;
2. Use of DRSM leads to a more accurate prediction of the mean flow field; its prediction on the fluctuating velocities however only bears qualitative resemblance to the measured distribution.
3. Particle dispersion model needs to be modified to allow the predicted particle tracks to follow the gas flow profile more closely at the horizontal duct's outer wall. Discrepancies between the measured and calculated gas velocities near-wall could also affect particle velocity predictions.

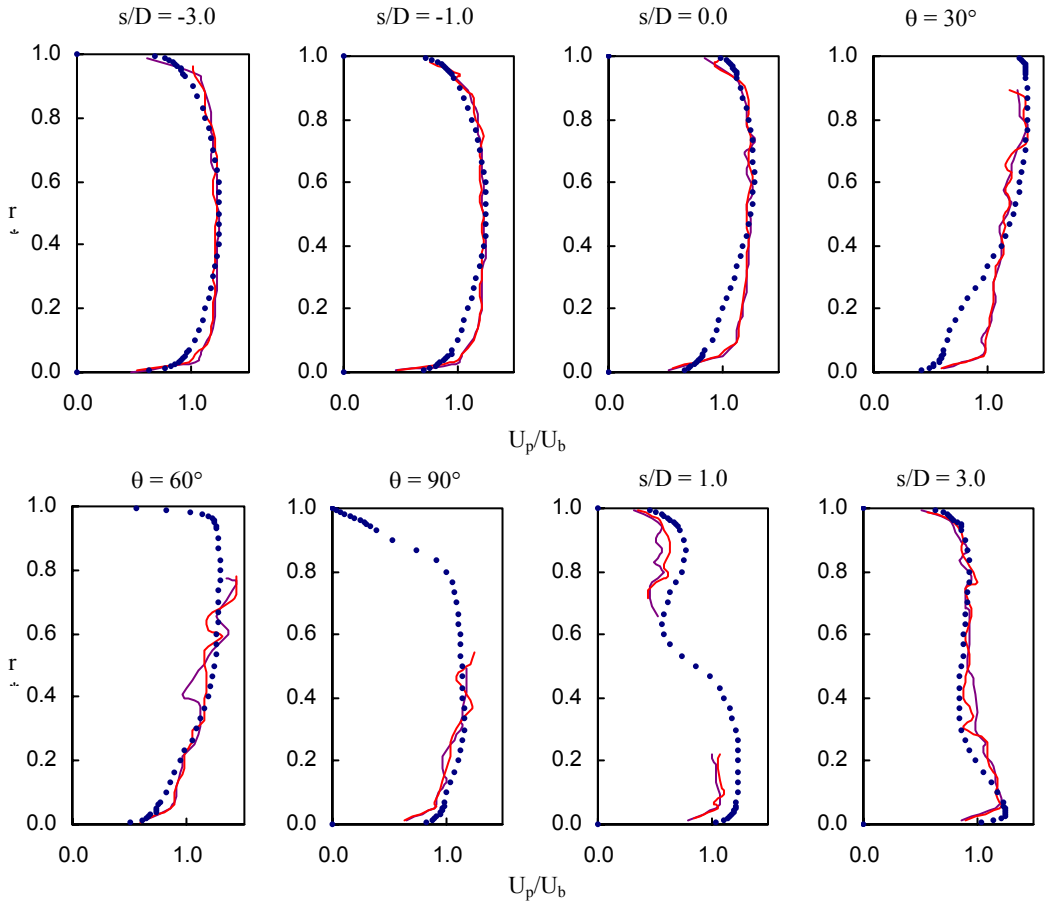

Figure 5: Normalised mean particle velocity profiles (• experiment; — uniform inlet profile; — fully-developed inlet profile)

ACKNOWLEDGEMENTS

The authors gratefully acknowledge the financial and other support received for this research from the CRC-Clean Power from Lignite, which is established and supported under the Australian Government's Cooperative Research Centre program.

REFERENCES

BARRATT, I.R., YAN, Y., BYRNE, B., and BRADLEY, M.S.A., (2000), "Mass flow measurement of pneumatically conveyed solids using radiometric sensors," *Flow Measurement and Instrumentation*, **11**, 223-235

BORGER, G.G., (1973), "The optimisation of wind tunnel contractions for the subsonic range," *PhD thesis*, Ruhr University, Germany

FAN, L.S., and ZHU, C., (1998), *Principles of gas-solid flows*, Cambridge University Press, Cambridge, UK

GOSMAN, A.D., and IOANNIDES, E., (1981), "Aspects of computer simulation of liquid-fuelled combustors," *AIAA paper no. 81-0323*

HUBER, N., and SOMMERFELD, M., (1998), "Modelling and numerical calculation of dilute-phase pneumatic conveying in pipe systems," *Powder Technology*, **99**, 90-101

KLIAFAS, Y., and HOLT, M., (1985), "Measurements of high-speed turbulent air flow in a 90° bend using laser-doppler velocimetry," *Applied Aerodynamics 3rd Conference*, Colorado Springs, Paper 85-4066.

LAUNDER, B., and SPALDING, D., (1974), "The numerical computation of turbulent flows," *Computer Methods in Applied Mechanics and Engineering*, **3**, 269-289

MA, J., and YAN, Y., (2000), "Design and evaluation of electrostatic sensors for the measurement of velocity of pneumatically conveyed solids," *Flow Measurement and Instrumentation*, **11**, 195-204

MILLEN, M.J., SOWERBY, B.D., COGHILL, P.J., TICKNER, J.R., KINGSLEY, R., and GRIMA, C., (2000), "Plant tests of an on-line multiple-pipe pulverized coal mass flow measuring system," *Flow Measurement and Instrumentation*, **11**, 153-158

SUDO, K., SUMIDA, M., and HIBARA, H., (2001), "Experimental investigation on turbulent flow in a square-sectioned 90-degree bend," *Experiments in Fluids*, **30**, 246-252

YAN, Y., BYRNE, B., and COULTHARD, J., (1995), "Sensing field homogeneity in mass flow rate measurement of pneumatically conveyed solids," *Flow Measurement and Instrumentation*, **6**, 115-119

YILMAZ, A., and LEVY, E. K., (1998), "Roping phenomena in pulverized coal conveying lines," *Powder Technology*, **95**, 43-48